12-2022

The effects of tubulin post-translational modifications on the flagellar motility of Trypanosoma brucei

Katherine Wentworth
kwentwo@g.clemson.edu

THE EFFECTS OF TUBULIN POST-TRANSLATIONAL MODIFICATIONS ON THE FLAGELLAR MOTILITY OF *TRYPANOSOMA BRUCEI*

A Thesis
Presented to
the Graduate School of
Clemson University

In Partial Fulfillment
of the Requirements for the Degree
Master of Science
Microbiology

---

by
Katherine Charlotte Wentworth
December 2022

Accepted by:
Joshua Alper, Committee Chair
Zhicheng Dou, Committee Co-chair
Kimberly Paul
Lesly Temesvari
James Morris

ABSTRACT

Trypanosoma brucei is a parasitic kinetoplastid that causes African trypanosomiasis and is transmitted to a mammalian host by the tsetse fly (*Glossina spp.*). *T. brucei* relies on its flagellar motility to carry out its morphological changes from the procyclic form (predominant in the fly vector) to the bloodstream form (infectious form in mammals) and navigate the bloodstream of its host. The driving structure within the flagellum is the axoneme, which is composed of microtubules and dynein motor proteins. The tubulin code hypothesis suggests that cells regulate microtubule motor protein activity through post-translational modifications (PTMs) of alpha and beta tubulin. However, the regulatory role of tubulin PTMs on the flagellar beat and structural effects on the subpellicular microtubules that dictate *T. brucei*'s unique morphology remain largely unknown. To characterize the importance of tubulin PTMs, I targeted the enzymes responsible for tubulin acetylation (alpha-tubulin acetyltransferase 1) and detyrosination (vasohibin) using two different strategies. First, we generated knockdowns of both enzymes through a well-developed RNAi system using the pZJM vector which revealed a >50% decrease in transcript and PTM presence. Second, we modified a CRISPR/Cas9 system to knock out both enzymes to compare gene expression and modification presence between cell lines. RT-qPCR and western blot analysis revealed complete absence of PTM enzyme transcripts and PTM presence in whole cell lysate. Confocal immunofluorescence revealed the subpellicular microtubules are highly acetylated and detyrosinated. Cell tracking and sedimentation assays revealed a significant increase in motility and swimming speed in non-acetylated cell lines. However, cells containing heavily tyrosinated

microtubules displayed an insignificant motility decrease in comparison to wild type. These results indicate acetylation negatively-regulates the dynein-driven flagellar motility of *T. brucei*, whereas detyrosination as little to no effect. Additionally, the subpellicular-microtubule array is significantly disrupted in the absence of acetylated alpha tubulin, leading to an elongated trypanosome (>14 μm). Overall, the findings from this study support the evolutionary conservation of tubulin PTMs in simple eukaryotes, such as *T. brucei*, and thus, can be expanded to similar *Leishmania* and *Trypanosoma* species.

ACKNOWLEDGEMENTS

This work was supported by the National Institute of Allergy and Infectious Diseases (NIAID) of the National Institutes of Health under award number R15AI137979 and the National Institute of General Medical Sciences (NIGMS) of the National Institutes of Health under award number P20GM109094. Additional funding was provided by the Clemson University Division of Research, College of Science, Department of Physics and Astronomy, Creative Inquiry program, and University Professional Internship and Co-op Program. We also acknowledge Jim Morris (Clemson University), members of the J. Morris Lab and Meredith Morris (Clemson University), for various reagents and samples, use of their equipment, and general advice.

TABLE OF CONTENTS

LIST OF FIGURES

LIST OF TABLES

CHAPTER ONE

LITERATURE REVIEW AND RATIONALE

1.1 *TRYPANOSOMA BRUCEI*

1.1.1 Life cycle

Trypanosoma brucei is a parasitic kinetoplastid that causes African trypanosomiasis, a disease commonly known as African sleeping sickness. The parasite is transmitted to a mammalian host by the tsetse fly (*Glossina spp.*).[5] During the transmission process, the morphology of the parasite significantly changes as it moves from colonizing the midgut of the fly (referred to as procyclic form (PCF)) to the salivary glands (metacyclic, visualized in Figure 1.1).[5] These morphological changes are depicted in Figure 1.1 and mostly attributed to pH, nutrient availability, and the vector's immune response.[22] In the bloodstream, the cellular morphology is short and stump, prior to reverting to PCF that colonizes the fly vector.[22] The cell changes morphology when unfavorable conditions are present, such as anti-parasitic drug treatment, host immune response activation, and nutrient depletion.[22] Thus, at any given life cycle stage, there is approximately a 20-30% variation in the phenotypes present.[22] Therefore, determining life cycle stage solely based on the observed phenotype requires a larger sample size (i.e., n > 100).

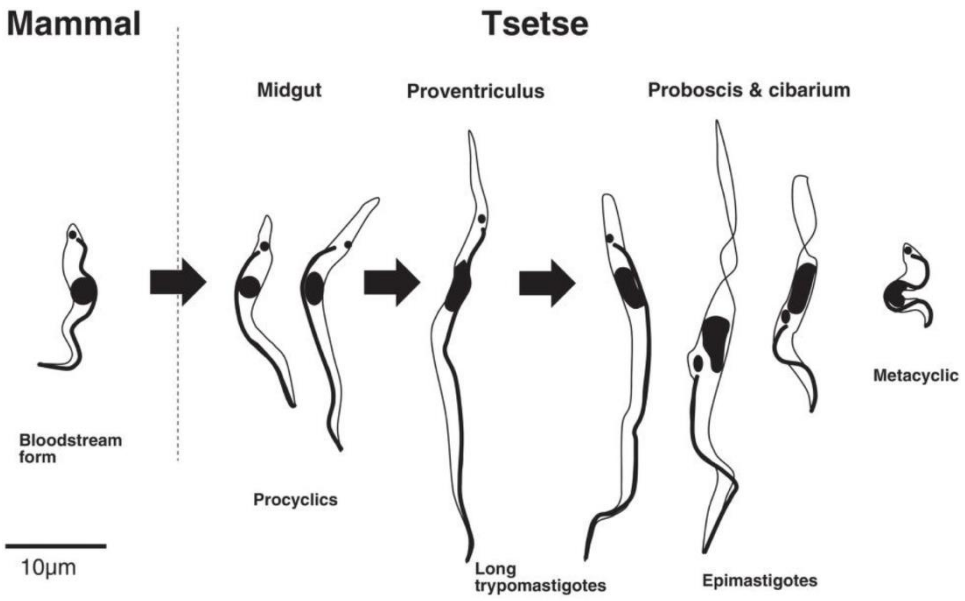

Figure 1.1: The *T. brucei* life cycle is governed by distinct environmental cues.[47] Sourced unmodified image under Creative Commons license CC BY 2.0 https://creativecommons.org/licenses/by/2.0/legalcode

1.1.2 Effectors of pathogenicity

The motility of *T. brucei* together with its variant surface glycoprotein (VSG) coating create a highly pathogenic parasite capable of crossing the blood-brain barrier and invading the central nervous system (CNS) of the host.[41] Upon colonization of the tsetse fly salivary gland, cellular division is halted and metacyclic VSG genes are expressed.[41] This protein coating replaces the procyclic acidic repetitive protein (PARP) coat and comprises ~95% of the membrane proteome.[41] VSG genes encode a GPI-anchored glycoprotein that is exported to the cellular membrane and rapidly cycled towards the flagellar pocket where it is endocytosed and recycled to the surface.[41] Rapid cycling in the membrane permits removal of host antibodies such as IgG, which can partially penetrate into and bind the VSG coat.[41] Upon endocytosis bound antibody is degraded, thus, evading

macrophage activation.[41] However, only one VSG variant is expressed at a time and as more macrophages recognize the VSG antigen, the parasite is cleared from the blood. To avoid dying off, one method the parasite can employ is switching which VSG gene is being expressed through activation of a different telomeric bloodstream expression site (BES).[41] This results in waves of parasitemia in the blood, with the host immune system never fully clearing the infection.[41]

Prolonged parasitemia in the blood is likely to result in parasite infection of the host CNS, which is almost always fatal.[42] Concentration of parasites near the blood-brain barrier (BBB), commonly characterized as a layer of microvascular endothelial cells intermixed with neuronal cell types) will result in penetration and subsequent disruption of this barrier. One *in vitro* study found ~10 parasites per 13 second interval could penetrate membrane pore sizes of ~1.4 μm.[39] This correlates with murine models exhibiting exponential parasitemia in the CNS after one week post-infection.[42] The observation of micro-pore invasion and an uninhibited velocity of bloodstream form (BSF) parasites at ~160 μm/s indicates any flagellar motility defect would drastically affect *T. brucei* pathogenesis.[39] Micro-pore invasion is critical for BBB invasion and requires constant swimming to cross this membrane. Therefore, interfering with the motility of the parasite will significantly impact the ability to cause the most severe effects of parasitemia in the CNS.

1.1.3 Intraflagellar motility mechanism

To navigate the bloodstream of its host, *T. brucei* relies on a unique motility mechanism: the flagellum beats with a bending waveform that alternates between base-to-

tip and tip-to-base propagation. The axoneme, a structure composed of microtubules and motor proteins, is responsible for driving the flagellar beat.[7] Microtubules are cylindrical tubes composed of individual protofilaments of repeating tubulin dimers, with each dimer composed of an alpha and beta tubulin subunit.[7] The axoneme has a signature microtubule 9+2 arrangement where 9 doublet microtubules surround a central pair (2) of microtubules in the center of the filament.[7] Axonemal dynein is the predominant motor protein within the axoneme that binds between microtubule pairs and generates the flagellar waveform through microtubule sliding.[7] Notably, axonemal dynein does not require similar activators to cytoplasmic dynein, such as dynactin (responsible for cargo binding), to generate force.[43] Axonemal dyneins generate a power stroke (the release and reattachment of the microtubule binding domains to tubulin subunits along the microtubule) through heavy chain release from tubulin dimers upon ATP hydrolysis and ADP release from the ATPase AAA+ motor domain.[43] The classical 9+2 arrangement of microtubule doublets in the axoneme is dictated by nexin linkers and inner and outer dynein arms (IDA and ODA). ODAs have a single, large motor that repeats every 24 nm and is largely responsible for flagellar beat frequency.[43] In contrast, IDAs have seven smaller motors that repeat every 96 nm and are considered to determine the flagellar beat amplitude.[43]

1.1.4 Importance of the subpellicular microtubule array in the T. brucei life cycle

Morphological changes occurring during the parasitic life cycle are governed by cytoskeletal network organization and flagellar modifications.[39] The subpellicular microtubule array (SPM) is a cross-linked network of microtubules underneath the plasma

membrane with at least three subdomains (Figure 1.2).[39,40] These subdomains have been noted to recruit different microtubule-associated proteins (MAPs), such as PAVE1/2, Tb927.9.10790, Tb927.11.1840 and, most notably, TbAIR9, which is critical for the integrity and organization of the entire SPM (Fig. 1.2). [40] Since all alpha and beta tubulin in *T. brucei* are from a single gene, subdomains marked by MAPs could serve as regulatory signals of intracellular trafficking due to the lack of different tubulin isoforms dictating domains of the cell.[40] Additionally, the flagellum has been noted to significantly impact the SPM structure based on the waveform it is exhibiting.[39] Inter-microtubule spacing across the SPM is not rigid, but instead is highly variable based on which subdomain is exposed to the highest forces from the flagellar wave.[39] The positioning of the flagellar axoneme is also flexible along the SPM, indicating that the entire array requires some level of plasticity based on the vigorous motility of the flagellum.[39] Throughout the life cycle, the cell changes its motility depending on where it is localized. When the cell is colonizing the midgut of the fly and migrates to the salivary gland, the epimastigote (phenotype of cells that have escaped the midgut into the proventriculus) is mostly adherent to the epithelium, which contrasts to the increased persistent swimming of slender BSF cells navigating the bloodstream of the host.[22] Therefore, response to environmental changes via chemotaxis can directly regulate the morphology of the cell and, thus, produce multiple phenotypes.

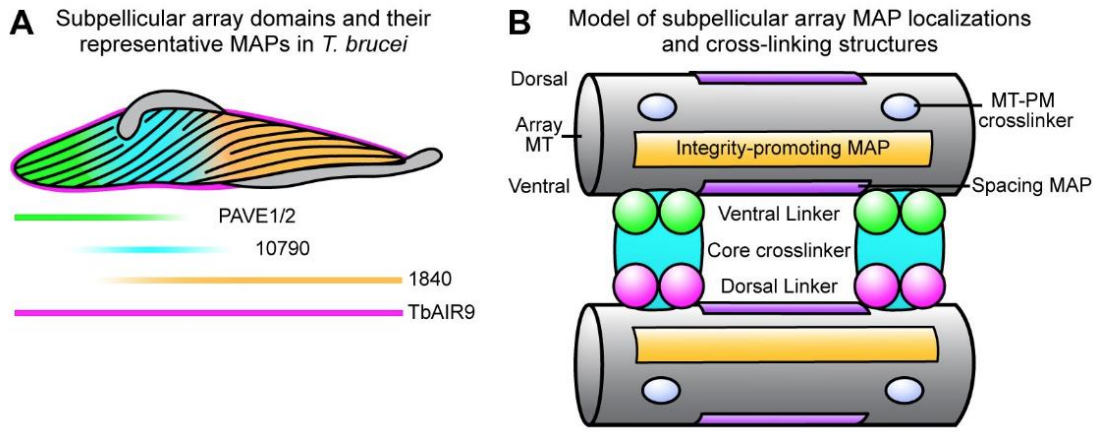

Figure 1.2: The subpellicular microtubule array is divided into distinct subdomains based on linker presence.[40] A. Relative localization of subpellicular array MAPs.[40] B. Cartoon representation of proteins involved in network crosslinking.[40] Sourced unmodified image under Creative Commons license CC BY 4.0 https://creativecommons.org/licenses/by/4.0/legalcode

1.2 Post-translational modifications of tubulin

Eukaryotes can indirectly regulate the activity of dynein by post-translationally modifying the tubulin dimers of the microtubules.[4,8] These modifications serve as molecular markers for subpopulations of tubulin or polymerized microtubules, in addition to recruitment of microtubule stabilizing MAPs.[4,8] Due to the direct interaction between the microtubule binding domain of axonemal dynein and the external microtubule doublet interface, tubulin PTMs are thought to significantly affect the processivity of axonemal dynein through different mechanisms.

1.2.1 Polyglycylation of alpha and beta tubulin

One type of tubulin PTM is polyglycylation, which is defined as the addition of several glycine residues on the C-terminal side tails of both alpha and beta tubulin by two

tubulin ligase-like proteins Ttll3 and Ttll8.[17] When polyglycylation is absent (*Ttll3/8*$^{-/-}$ mice), these sites are heavily polyglutamylated, indicating enzymatic competition. In these knock outs, when a murine sperm cell would encounter a barrier it would exhibit planar, circular movement instead of processive helicoidal swimming, which is denoted by the cell moving along a single vector. Processive motility could still occur but if the cell encountered an obstacle it could not correct its position or respond properly to chemotaxis signals. Knock out mice had a 25% fertility success rate in comparison to wild type mice, indicating severely reduced sperm cell motility.[17] These results indicate that indirect dynein regulation by tubulin PTMs is critical for processive motility in eukaryotic cells.

1.2.2 Alpha tubulin acetylation

A tubulin PTM that does not interact with the C terminal tail is the acetylation of the luminal (internal portion of the microtubule) lysine 40 residue on alpha tubulin. Acetylation is carried out by the enzyme alpha-tubulin acetyltransferase 1 (αTAT1).[4] Researchers agree that polymerized microtubules, not individual dimers, are acetylated by αTAT1.[8] If acetylated tubulin dimers are re-polymerized *in vitro*, the spontaneous microtubule nucleation rate (formation of new microtubules from single tubulin dimers) decreases 2.7-fold in comparison to non-acetylated dimers.[8]

Compared to PTMs such as polyglycylation that affect the C-terminal tail, acetylation occurs on the inner luminal side of the microtubule lattice in between adjacent tubulin dimers. Since this modification could affect the microtubule structure, research is divided on the topic of acetylation's impact on microtubule stability. To understand how

acetylated versus non-acetylated microtubules respond to continuous mechanical stress, Portran *et al.* bound both types of microtubules to a glass substrate which would rotate to simulate flagellar rotation.[10] Acetylated microtubules were able to endure repeated mechanical stress and maintain their original structure in comparison to non-acetylated microtubules.[10] They concluded that acetylation weakens the lateral contacts between tubulin dimers, permitting elasticity of an otherwise rigid filament. A supporting study found that tubulin acetylation increases intra-dimer spacing by ~ 8 Å and is significant enough to yield new mechanical properties to allow the microtubule lattice to bend freely and endure the repeated mechanical stress of the beating flagellum.[44] Additionally, acetylation has been observed to increase dynein processivity *in vitro* when compared to deacetylated microtubules.[8] Therefore, acetylation serves to stabilize microtubules under high mechanical stress from dynein.

1.2.3 Alpha tubulin detyrosination

Conversely, the detyrosination of alpha tubulin yields more subtle effects. Vasohibin 1 is observed to cleave the endogenous C-terminal tyrosine of alpha tubulin upon incorporation into the microtubule lattice, where the majority of the protofilament is detyrosinated and the polymerizing tip contains primarily tyrosinated tubulin.[4,8] Recycling of detyrosinated tubulin dimers is possible via the tyrosination activity of tubulin-tyrosine ligase.[4] Structurally, this single residue removal does not affect the tubulin dimer spacing, but instead is considered to serve as a molecular signal to MAPs and motor proteins binding to the external microtubule surface.[4,8]

This modification is alpha tubulin-specific due to the observation that when the alpha tubulin C-terminal tail is cleaved the dynein processivity decreases by approximately 85% in comparison to the cleavage of only the beta tubulin tail (20% decrease).[8] However, if half of the microtubule (constructed *in vitro*) had tyrosinated alpha tubulin to bind to but would eventually cross over onto a region of detyrosinated tubulin, the processivity stayed the same.[8] This indicates that tyrosinated tubulin is necessary for the binding and start of dynein processivity but is not required for the duration of the run along the microtubule.[8]

1.2.4 Tubulin Acetylation and Detyrosination in T. brucei

Immunofluorescence of the *T. brucei* flagellum revealed that mature flagella are largely detyrosinated and acetylated (Figure 1.3).[9] Since all tubulin is the same homolog in *T. brucei*, the microtubules within the cytosol and SPM were also observed to be post-translationally modified.[9] A unique phenotype observed for *TbVASH* (*T. brucei*, vasohibin) knockdown mutants was problems with late-stage cytokinesis.[9] Cells could complete the majority of cell division, including nuclear and kinetoplast (subcellular concentration of mitochondrial DNA) division, but were connected at the distal tip for a prolonged period prior to separating, or they never fully divided and formed clusters.[9] Therefore, we could observe a potential cellular division defect.

Most recently, van der Laan *et al.*. published an analysis of the effects of using CRISPR/Cas9 to knock out vasohibin in *T. brucei*.[49] Interestingly, through western blot probing they discovered that *TbVASH* detyrosinated the C-terminal tail of both alpha-tubulin and beta-tubulin.[49] Upon knock out, they observed an enhanced number of clusters

in comparison to wild type, which correlates with the previous knockdown phenotype having difficulties with late-stage cytokinesis.[49] Additionally, the majority of wild type *T. brucei* were of length 4-8 μm compared to vasohibin knock outs averaging 8-12 μm in length.[49] However, the authors concluded that the motility of the *T. brucei* cells was not affected despite the morphological defects due to the lack of observable microtubule or dynein structural differences in cryo-EM cross sections of the flagellum.[49] To further characterize the vasohibin knock outs, we will investigate the cell motility phenotype through cellular motility tracking assays.

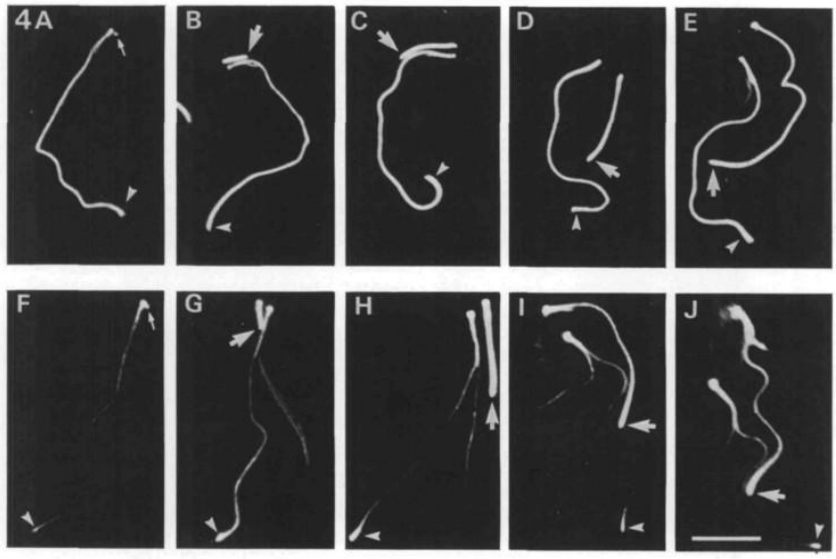

Figure 1.3: Post-translationally modified tubulin is present in the flagellum of *T. brucei*.[9] Immunofluorescence of acetylated (A-E) and detyrosinated (F-J) alpha tubulin in *T. brucei*.[9] A and F indicate a single cell prior to division; E and J indicate completed cellular division. Full arrows denote newly-formed flagellum; arrowheads denote mature flagellum ends. Reproduced unmodified image from the Journal of Cell Science.[9]

1.3 Expression modification systems in *T. brucei*

1.3.1 RNA interference

Since the late 1990s, RNA interference (RNAi) has been the primary method of modifying protein expression in *T. brucei*.[45] This mechanism works where the *T. brucei* argonaute protein, TbAGO1, recognizing double-stranded RNA and degrading matching mRNAs through its endonuclease function.[45] TbAGO1 degrades foreign mRNA that could act as a retroposon.[45] Early studies transfected dsRNA into *T. brucei* to achieve degradation of their target transcripts.[14] However, due to the unstable nature of RNA and the necessity for multiple electroporations, incorporation of a DNA construct that generated dsRNA was adopted.[14]

The vector used in my thesis work is the pZJM vector, which generates dsRNA upon tetracycline addition.[29] The pZJM vector contains a phleomycin selection marker and a chromosomal integration site at the silent rRNA spacer locus.[29] In brief, a 200-300 bp section of the target gene is PCR-amplified and ligated in between two opposing T7 promoters with downstream tetracycline-repressor binding sites.[29] This portion is inserted in between sequences that generate a dsRNA structure upon transcription.[29] Therefore, upon tetracycline addition to the media, cells will generate dsRNA against the transcript of interest and target the cognate mRNAs for degradation.

1.3.2 CRISPR/Cas9

CRISPR is an acronym for Clustered Regularly Interspaced Short Palindromic repeats that are derived from bacteriophages that had previously infected a bacterial cell.[14] These sequences are recognized by Cas endonucleases, which can generate a double stranded break slightly upstream of a Protospacer Adjacent Motif (PAM). The Cas9 endonuclease recognizes the PAM sequence 5' – N-G-G – 3', which is highly favorable for use in eukaryotic organisms.[14] Additionally, the Cas9 sequence, derived from *Streptococcus pyogenes*, has been adapted for use in human, murine, and numerous other eukaryotic cell lines.[14]

Double-stranded DNA breaks are the most difficult for *T. brucei* to repair since the DNA polymerase has no repair template and thus, non-homologous end joining (NHEJ) typically occurs. [14,46] NHEJ is the rapid repair of a double-stranded break through random indel (nucleotide insertion or deletion) production between the breaks.[14,46] This is not ideal, as the NHEJ mechanism, is error-prone, however, this process renders the gene replicable for the polymerase. However, in synthetic biology this is favorable since the gene will have a potential stop codon, frameshift mutation, or residue addition that changes the protein conformation. Besides NHEJ, homology-directed repair (HDR) can occur in diploid eukaryotes, such as *T. brucei*, where if one allele is spliced by Cas9 the other allele can serve as a template.[14,46] This is not favorable for production of random knock outs, but can be useful if a repair template is provided to permit recombination of a user-defined mutation.

CRISPR/Cas9 modification systems were not published for use in *T. brucei* until after 2015. In 2017, Beneke *et al.*. produced the pT and pPLOT vector system, optimized for fluorescent tag and antibiotic resistance insertion.[46] This system coincided with the open source LeishGEdit software that generates optimal target sequences and primer sets for this system based on the kinetoplastid species genome and target gene.[46] The authors targeted the GPI-anchor for VSG, one of the *T. brucei*'s key virulence factors in BSF cells. Gel electrophoresis indicated successful knock outs, and knock out cells contained large quantities of free VSG in the cell lysate supernatant. [46]

In early 2018, Rico *et al.*. published their pT7sgRNA and pRPaCas9 vector system.[14] In this study, the authors tested the effectivity of their system by designing 20bp targets against the AQP2 gene (aquaporin 2) which, when mutated, permits resistance to pentamidine. This allowed efficient screening of randomly generated knock outs with pentamidine selection.[14] They also provided a ssDNA repair template with a point mutation to generate a PmlI cut site, visualized by gel electrophoresis and genomic sequencing, to ensure specific nucleotides can be modified.[14] This system indicated double-allelic knock outs can be generated in *T. brucei* through random indel mutations or specific nucleotide changes.

1.3.3 Application Comparison

Both knockdown and knock out methodologies reduce protein expression, however, deciding which method to use depends on the expected phenotype. The use of RNAi is favorable when working with *T. brucei* cell culture since expression levels of the

target gene are typically reduced by 60-80% compared to wild type and permits analysis of a lethal phenotype.[29] However, this mechanism is considered to be 'leaky' since a full knockdown phenotype (absolute elimination of target mRNA) would require constant binding of TbAGO1 to the target transcript. Thus, partial expression of the target gene is possible and could yield a subtle wild type phenotype. This might not be a concern for a target with a visible phenotype, such as flagellar attachment protein 3 (FLAM3) that is responsible for anchoring the flagellum of *T. brucei* to the cell body. The characteristic FLAM3 knockdown phenotype is observed when the is completely detached from the cell body; thus, partial expression of the wild type mRNA would be visible by microscopy as an attached flagellum. With gene targets that have unknown or subtle phenotypes, partial wild type expression might interfere with observing a mutant phenotype.

CRISPR/Cas9 mutations are permanent, which is beneficial as the cells no longer require induction, and can be maintained almost indefinitely. Additionally, a total expression knock out will eliminate the concern for partial wild type phenotype presentation. Any phenotype remaining after knock out would indicate the presence of a redundant gene. Such is the case of tubulin polyglycylation, where knocking out only one tubulin tyrosine ligase-like enzyme (3 or 8) will still produce fully polyglycylated microtubules.[17] However, the CRISPR/Cas9 system is fairly new to the *T. brucei* community, where the primary technical concern revolves around screening. Without using a screenable phenotype, such as fluorescence or antibiotic resistance, finding a clone is similar to finding a needle in a haystack. This is a significant deterrent in using this system over RNAi in many studies, unless a repair template is being used. The issue with a repair

template is that since *T. brucei* is a diploid organism, a single allele knock out and subsequent knock-in will produce resistant clones that still have one functional gene copy. However, to use two repair templates with different resistance markers in a cell line that is most likely already under drug selection is not ideal as this would put pressure on the cellular growth and mask potential knock out growth phenotypes.

1.4 Rationale

In this study, we sought to investigate eukaryotic motility regulation in the model organism, *T. brucei*. Our hypothesis is that if axonemal tubulin was not post-translationally modified, regulation of axonemal dynein would be disrupted and thus, the flagellum of *T. brucei* would not generate its unique waveform. We investigated the effects of indirect dynein regulation on the flagellar motility of *T. brucei* through two tubulin PTMs, acetylation and detyrosination. We utilized a primarily *in vivo* approach to determining the effects of PTMs on motility through the quantification of swimming behavior and sedimentation rates of the *T. brucei* alpha tubulin acetyltransferase 1 (Tb927.3.1400, hereafter referred to as *TbαTAT1*) and vasohibin (Tb927.11.1060, hereafter referred to as *TbVASH*) knockdowns and knock outs. Based on previous observations, we expected the removal of *TbαTAT1* and *TbVASH* would significantly impact the motility of *T. brucei*. Disruption of tubulin acetylation leads to increased, unregulated motility in comparison to the subtle decrease in persistence of cells with highly tyrosinated tubulin.[9] Therefore, we expect a more severe motility defect in *TbαTAT1* mutants compared to *TbVASH* mutants. Quantifying the effects of tubulin PTMs on whole cell motility is an indirect measurement of dynein processivity; thus, continuation of this study would include *in vitro* quantification

of axonemal dynein motility on differing modified tubulin substrates. The results of this study will expand our understanding of tubulin PTMs in different eukaryotic species in addition to how regulation of the flagellar motility of *T. brucei* impacts its pathogenesis.

CHAPTER TWO

MATERIALS AND METHODS

2.1 Cell Culturing

We cultured 29-13 *T. brucei* brucei (a gift from the Jim Morris Lab, derived from strain Lister 427) as the parental cell line for all experiments in this study. The 29-13 cell line encodes an integrated T7 polymerase under geneticin selection (G418; 15 μg/mL) and a tetracycline repressor under hygromycin (50 μg/mL) selection for induced gene expression.[23] Growth medium consisted of SDM-79 (custom produced by Life Sciences Research Products, Thermo Fisher Scientific for the Eukaryotic Pathogens Innovation Center Labs, Clemson University, Clemson, SC) supplemented with 10% (v/v) heat-inactivated tetracycline-free fetal bovine serum (S162TA, Biowest, MO) and porcine hemin (7.5 μg/mL; AAA11165-03, Alfa Aesar, MA).[24] We maintained cells at a 1:10 passage in 5 mL total volume every 48 hrs to yield a logarithmic growth phase between 1×10^6 and 1×10^7 cells/mL (in a humidified incubator 27 °C, 5% CO_2).[25]

2.2 RNAi constructs and Cloning Strategy

To knock down the expression of targeted genes in trypanosomes, we used the tetracycline-inducible pZJM RNAi vector.[29] To generate pZJM-αTAT1 (Fig. A1.1) we

excised the alpha tubulin gene from the pZJM-tubulin vector (a gift from James Morris, Clemson University) using XhoI (R0146S, New England Biolabs, MA) and HindIII (R3104S, New England Biolabs, MA) restriction enzymes and inserted a 269 bp fragment of αTAT1 (Tb927.3.1400[19]) PCR amplified from 29-13 *T. brucei* gDNA. To generate pZJM-VASH (Fig. A1.2), we used the linearized pZJM vector and ligated in a 173 bp fragment of VASH (Tb927.11.1060[19]) from the 3'-UTR that we PCR amplified from 29-13 *T. brucei* gDNA.

Our transfection strategy for all cell lines, in brief, involved pelleting 5.0 x 10^7 total 29-13 *T. brucei* cells, washing and resuspending in 400 μL cytomix (1 M KCl, 1 M $CaCl_2$, 0.5 M KH_2PO_4, 1 M HEPES (pH = 7.6), 0.5 M EGTA, 1 M $MgCl_2$, 0.5% (w/v) D-glucose, 0.01% (v/v) BSA, 1 mM hypoxanthine)[30] with 40 μg of pZJM-αTAT1 and pZJM-VASH linearized with NotI (R0189S, New England Biolabs, MA) and electroporated twice at 10 s intervals (1.5 kV, exponential decay, 25 μF, 4 mm cuvette).[30] We conducted each transfection alongside a negative control with vector substituted by 1X PBS to monitor cell growth in response to selection. After 24 hrs, flasks were supplemented with phleomycin (5 μg/mL) to select for cells containing the pZJM vector. Cells exhibiting log phase growth were diluted to 0.5 cells/well in 500 μL of 1:1 mixture of conditioned and fresh media in a 24-well plate to isolate clonal transfects. We used conditioned media to provide optimal growth conditions during dilution cloning. We prepared conditioned media by filtering supernatant from 1.0 x 10^7 cells/mL 29-13 *T. brucei* culture through a 0.2 μm PTFE filter. Wells were monitored daily for growth (over 10-14 days). Positive wells were induced with doxycycline (1 μg/mL) for 96 hrs prior to RT-qPCR and Western blot analysis.

2.3 CRISPR/Cas9 constructs and Cloning Strategy

To generate random indel mutation knock outs, we transfected tetracycline inducible-Cas9 29-13 *T. brucei* cells (a gift from the Jim Morris Lab) with our modified pT7sgRNA vector (vector provided by the David Horn Lab), pT7sgRNA-BLAST. We excised the phleomycin resistance cassette with MluI and BamHI and replaced with our custom blasticidin gene which contains the promoter overhangs removed by the digestion with MluI, yielding the pT7sgRNA-BLAST vector. We designed 20 bp guide RNA target sequences through EuPaGDT[2] for *TbαTAT1* and *TbVASH*. Target sequences were ligated into the pT7sgRNA-BLAST vector via inverted repeat BbsI restriction sites between a T7 promoter sequence and the guide RNA scaffold region to generate pT7-αTAT1 and pT7-VASH constructs (Fig. B1.1 in Appendix B).

We followed the pZJM transfection protocol for pT7sgRNA-BLAST with the exception of cells being constantly maintained in phleomycin (5μg/mL) to maintain the Cas9 vector. After 24 hrs post electroporation, flasks were supplemented with blasticidin (20 μg/mL) to select for cells containing the pT7sgRNA-BLAST vector. Cells exhibiting log phase growth were induced with doxycycline (1 μg/mL) for 96 hrs prior cloning to induce Cas9 expression. Induced cells were diluted to 0.5 cells/well in 100 μL of 1:1 conditional to fresh media without doxycycline in two 96-well plates to isolate clonal transfects. Wells were monitored daily for growth over 10-14 days. Positive wells were passed into 500 μL fresh media in a 24-well plate prior to RT-qPCR, PCR, and Western blot analysis.

2.4 RT-qPCR

We extracted total RNA from 1.0-2.0 x 10^7 cells and treated the extract twice with DNase I to minimize gDNA contamination (T2010, New England Biolabs, MA). All RT-qPCR experiments used the Luna Universal One-Step RT-qPCR Kit (E3005L, New England Biolabs, MA) following the manufacturer's protocol for 20 μL reactions. The thermocycler program used a single reverse transcription step (10 min at 55 °C) and an initial denaturation (1 min at 95 °C), followed by 40 cycles of 15s denaturation and 30s extension (CFX96, Bio-Rad Laboratories, CA). We normalized relative expression of *TbαTAT1* and *TbVASH* to wild type and a housekeeping gene (alpha tubulin) using the ΔΔCq method.[31] Briefly, the equation used was $-2^{(\Delta Cq \text{ (treated sample)} - \Delta Cq \text{ (untreated sample)})}$ where the change in the Cq (quantification cycle) of the gene of interest to the Cq of the housekeeping gene was calculated for the treated sample (induced Cas9) and untreated sample (uninduced Cas9).[31]

2.5 Western blots

Whole cell lysates from 1.0x10^5 cells were incubated in 1X SDS-sample buffer at 95 °C and run in 10% SDS polyacrylamide gels for 35-45 min at 200 V in a mini-PROTEAN tetra vertical electrophoresis cell (Bio-Rad Laboratories, Inc). We transferred the protein bands onto PVDF membranes (170-4156, Bio-Rad Laboratories, Inc) with a Trans-Bolt Turbo System (Bio-Rad Laboratories, Inc), and allowed the membrane to air dry for 20 min. To analyze the presence of acetylated alpha tubulin, we incubated membranes in mouse clone 6-11 B-1 anti-acetylated tubulin primary antibody diluted

1:7500 in blocking buffer (1% (w/v) skimmed milk powder prepared in 1X PBS with 0.1% (v/v) Tween), washed thoroughly with PBST (0.1% (v/v) Tween in PBS), and incubated in alkaline phosphatase-conjugated goat anti-mouse secondary antibody (31328, Thermo Fisher Scientific) diluted to 1:5000 in blocking buffer. We detected the bound alkaline-phosphatase labeled antibodies by incubating the membrane in BCIP/NBT (5-bromo, 4-chloro, 3-indolylphosphate/nitro-blue tetrazolium, AMRESCO, LLC.) substrate for 15-20 min. Finally, we imaged the membrane using the BioRad ChemiDoc and quantified the bands with ImageJ.[20, 21] To analyze the presence of detyrosinated alpha tubulin, we incubated membranes in rabbit anti-detyrosinated tubulin primary antibody (AB3201, Sigma-Aldrich, MO) diluted to 1:2500 in blocking buffer and alkaline phosphatase-conjugated goat anti-rabbit (31342, Thermo Scientific, MA) secondary antibody diluted 1:5000 in blocking buffer.

2.6 Immunofluorescence

All immunofluorescence images were captured using the Leica TCS SPE confocal DM2500 microscope with a plan apochromat 63x oil-immersion objective (Leica, NA 1.40). We quantified and overlaid our images using ImageJ.[20,21] We fixed 2.0×10^6 total cells on a glass slide using 2% formaldehyde, rinsed them with ample wash solution (0.1% (w/v) normal goat serum, NGS, in 1X PBS) before applying a 0.1 M glycine solution to quench unreacted aldehydes.[32] After 15 min, we rinsed the cells with wash solution and permeabilized them with 0.5% (v/v) Triton-X 100 in 1X PBS. We washed the cells with

wash solution and added 50 μL of BioTracker 488 cell-permeable dye (SCT136, Sigma Aldrich). Finally, we sealed the sample with a coverslip and nail polish.

2.7 Sedimentation Assays

We measured the rate of sedimentation of our *T. brucei* cells lines measuring the absorbance at λ = 600 nm near the top of a cuvette.[26] To prevent recording light scattered by sedimented cells, we taped the bottom of the cuvette (~0.75 in) with black electrical tape to only permit light to pass through ~200 μL of the sample. We diluted 500 μL of log phase cells to a total of 1.0×10^6 cells into 1 mL disposable cuvettes (UVette, 952010051, Eppendorf AG, Hamburg, Germany). We measured the absorbance every hour for a total of 7 hrs using a spectrophotometer and repeated these trials in triplicate (V-1200 Spectrophotometer, 10037-434 VWR International, LLC). Two cuvettes were made for each cell line: one cuvette was kept undisturbed for maximum sedimentation and the other was manually stirred every hour to account for cell division.[26] We subtracted the absorbance of the stirred from the unstirred culture to yield a negative absorbance change due to the sedimentation of the cells over time.

2.8 Cell Tracking

To analyze the average speed and velocity of our cell lines, we tracked the paths of approximately 300 cells in 100 – 150 μm deep motility chambers constructed from parafilm that had been sealed between cleaned glass slides and 22 mm coverslips (16004-302, VWR).[34] We incubated each chamber with 0.25% poly-L-glutamate (P4886, 1133Sigma-

Aldrich, Inc.)[34] diluted in 1X PBS for 25 min to prevent cell adherence and rinsed the excess with distilled-deionized water and 70% ethanol.[34] We diluted cells to a final density of 1×10^6 cells/mL and added 10 μL into the motility chamber and recorded the cells with phase-contrast microscopy (Aus Jena Telaval 3 inverted binocular microscope) at 5x magnification (Aus Jena planachromat, NA 0.1). We recorded 10 second movies at 45 frames per second using a CCD camera (Grasshopper3 USB3 GS3-U3-15S5M-C, Teledyne FLIR, LLC.) We preprocessed the image sequences in ImageJ by subtracting the maximum projection from each frame and applied a spot-enhancing 2D filter (SpotTracker)[35,36] to clarify the image and reduce background noise.[22,23,35] We quantified motility by tracking single, non-intersecting cell paths to minimize the breaking of tracks using the wrmicrotubulerck[37] (1. Minimum 100 pixels^2 , 2. Maximum 400 pixels^2 , 3. threshMode: Otsu) and ParticleTracker[38] (Radius = 15 pixels; 3 pixels cutoff).

CHAPTER THREE

RESULTS

3.1 Generation of knock out and knockdown cell lines

We identified putative homologs of alpha-tubulin acetyltransferase 1 and vasohibin through the NCBI TriTryp database. The percent nucleotide identities for these enzymes were high (≥50%) when compared to other known sequences in *Trypanosoma spp.* and widespread throughout the coding region (Table A.1, Appendix A).[1] We generated knockdowns of both enzymes through a well-developed RNAi system using the tetracycline-inducible pZJM vector (Materials and Methods). Previous research indicated knockdown success when the 3' UTR is the target for mRNA silencing instead of the coding region.[18] Therefore, we initially targeted the 3' UTR of both genes, with success for *TbVASH*. For *TbαTAT1,* we targeted a central portion of the coding sequence (CDS) due to inefficient knockdown when we targeted the 3' UTR. We confirmed efficient knockdown populations through RT-qPCR and Western blots of cells grown in doxycycline for at least 96 hrs (Figure 3.1A-C). *TbαTAT1* transcript presence was reduced by >60% and correlated with a similar tubulin acetylation reduction. However, for the western blots it is important to note that the primary antibody used for detection of acetylated tubulin, 6-11 B-1, can detect deacetylated tubulin, but not tubulin that was never acetylated. Therefore, minimal band presence in lane 2 of Fig. 3.1C is expected. *TbVASH* transcript was reduced by 50% and tubulin detyrosination was reduced by approximately 33%. The close correlation in PTM presence to putative enzyme transcript indicated

TbαTAT1 and *TbVASH* are the primary enzymes capable of these tubulin modifications and there are no significant rescue mechanisms.

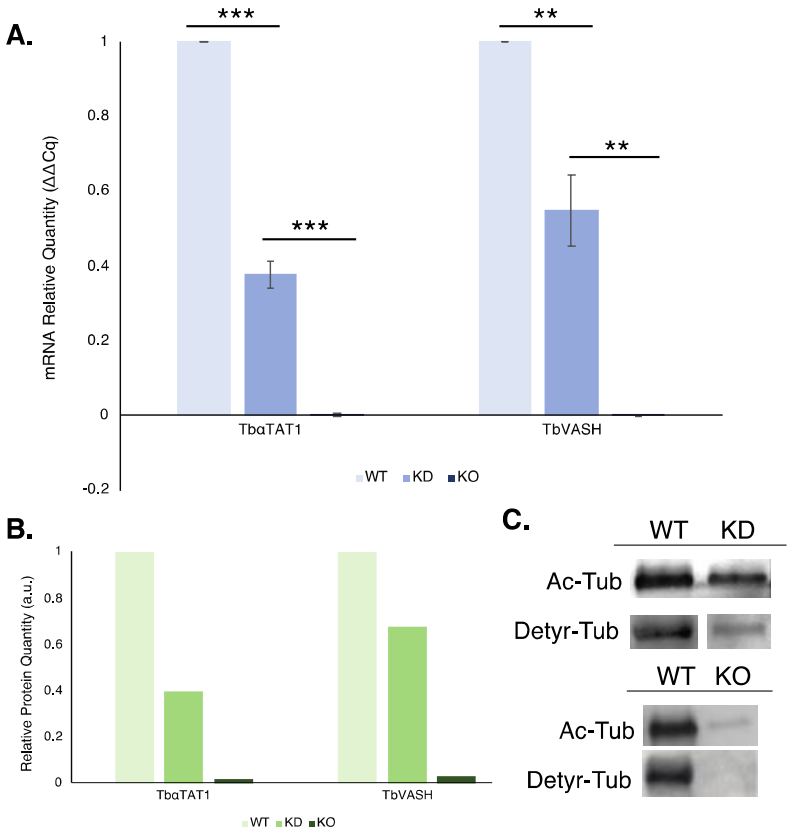

Figure 3.1: *TbαTAT1* and *TbVASH* knockdowns and knock outs correlate with tubulin PTM reduction. A. Relative mRNA quantification from average ΔΔCq calculations (Materials and Methods). Error bars are standard error of the mean (SEM, n = 3). Statistical significance determined by unpaired t-test (** = $p \leq 0.01$, *** = $p \leq 0.001$)B. Western blot band quantification through densitometry (Materials and Methods). C. Tubulin PTM presence in uninduced (WT), induced (KD), and knock out (KO) cell lines determined by western blot. Acetylated tubulin detected with 1:7500 primary antibody clone 6-11 B-1 anti-mouse; Detyrosinated tubulin detected with 1:2500 anti-detyrosinated alpha tubulin anti-rabbit primary antibody. Secondary antibodies diluted 1:5000 in blocking buffer (Materials and Methods).

Additionally, we utilized our modified CRISPR/Cas9 system to knock out both enzymes to compare gene expression and modification presence between cell lines. We modified the guide RNA vector (developed by the David Horn lab) and create a protocol similar to the one used for RNAi.[14] In brief, we changed the phleomycin resistance cassette in the sgRNA vector for a custom-designed blasticidin resistance gene and transfected this vector into cells containing integrated Cas9. Upon successful selection of a dense population in blasticidin, we induced the Cas9 expression with doxycycline for a minimum of 96 hrs to yield maximum knock out efficiency. We then diluted the population to 0.5/cells per well in a 96-well plate and growing isolates were screened via RT-qPCR and western blot after 10-15 days of growth. For both *Tbα**TAT1*** and *TbVASH*, relative transcript quantity was close to zero (<0.01) and minimal to no detectable PTM presence, indicating a double allele knock out (Figure 3.1A-C). The high correlation between transcript reduction and PTM presence suggests that a knock out cell line will have no modified tubulin.

3.2 Immunofluorescence reveals both the axoneme and SPM are post-translationally modified

Previously, immunofluorescence microscopy have indicated the microtubules of *T. brucei* are largely acetylated and detyrosinated.[9] We prepared slides with a 50:50 mixture of uninduced:induced *Tbα**TAT1*** and *TbVASH* knockdowns to assess fluorescence intensity across both cell lines in the same image, without bias. *Tbα**TAT1*** knockdowns have reduced anti-acetylated tubulin based on the dim peripheral outline of subpellicular microtubules in

the cellular cross section and appear to be elongated in comparison to their uninduced counterpart (Figure 3.2A). *TbVASH* uninduced cells have widespread detyrosinated tubulin and similar shape to the induced cells (Figure 3.2D). In both cell lines, induced and uninduced cells expressed similar fluorescence intensity of the opposite tubulin PTM (Figure 3.2B-C). However, the cytosolic availability of acetylated tubulin is reduced in comparison to detyrosinated tubulin based on the lack of emission in the cytoplasm of acetylated wild type cell culture. Our observations correlate with the current literature and highlight the dense acetylated tubulin presence in the subpellicular microtubule array.

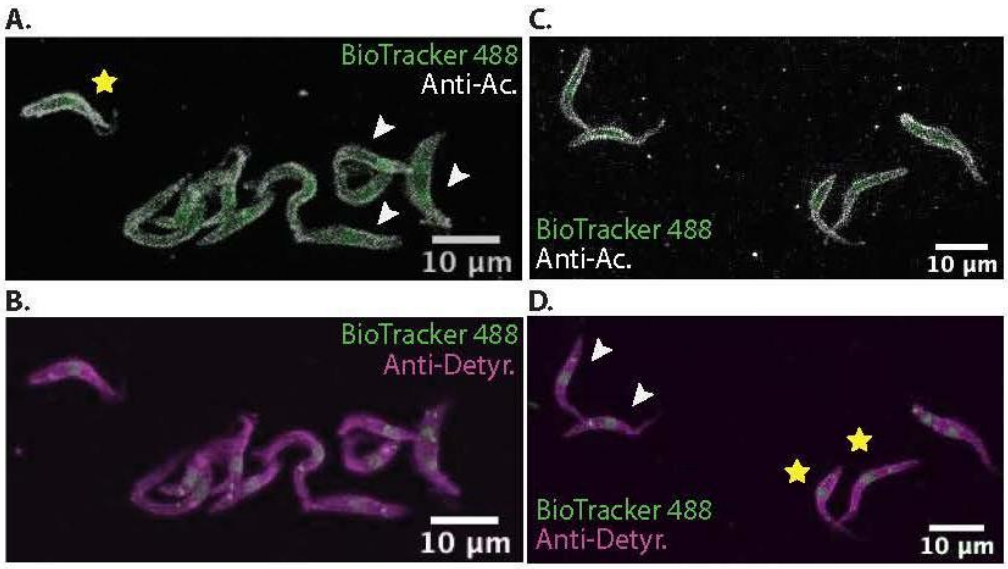

Figure 3.2: *T. brucei* subpellicular and axonemal microtubules are largely acetylated and detyrosinated. Confocal immunofluorescence with a 63x objective lens of uninduced (stars) and induced (arrowheads) pZJM-TbαTAT1 (A-B.) and pZJM-TbVASH (C-D.) mixed cultures. Primary and fluorescent secondary antibodies were diluted to 1:200 in NGS blocking buffer (Materials and Methods)

3.3 *TbαTAT1* induced cells, but not *TbVASH*, display increased speed and are resistant to sedimentation

To understand how the reduction of tubulin acetylation and detyrosination affect the motility of *T. brucei*, we tracked the average speed and average velocity of each cell line over 10 second intervals (Figure 3.3). The average velocity is calculated based on the displacement of the cell from the initial to final frame, which significantly increased for *TbαTAT1*, but not *TbVASH* cell lines upon induction (Figure 3.3A; unpaired t-test, $p = 0.0023$, $p = 0.2598$, respectively). Additionally, induced *TbαTAT1* culture experienced a significant velocity increase of 2.347 ± 0.537 μm/s compared to induced *TbVASH* culture. The average speed is calculated from the total path length of the cell over time, which reveals if the cell is experiencing a higher running or tumbling frequency. A similar increase in speed is noted for *TbαTAT1* induced cells (1.837 ± 0.490 μm/s), however, the change in speed for *TbVASH* cells was not significant (Figure 3.3B; unpaired t-test, $p = 0.0042$, $p = 0.652$, respectively). Therefore, induction of RNAi significantly increased the speed and velocity of *TbαTAT1* cells, but no significant changes were observed for *TbVASH* cells.

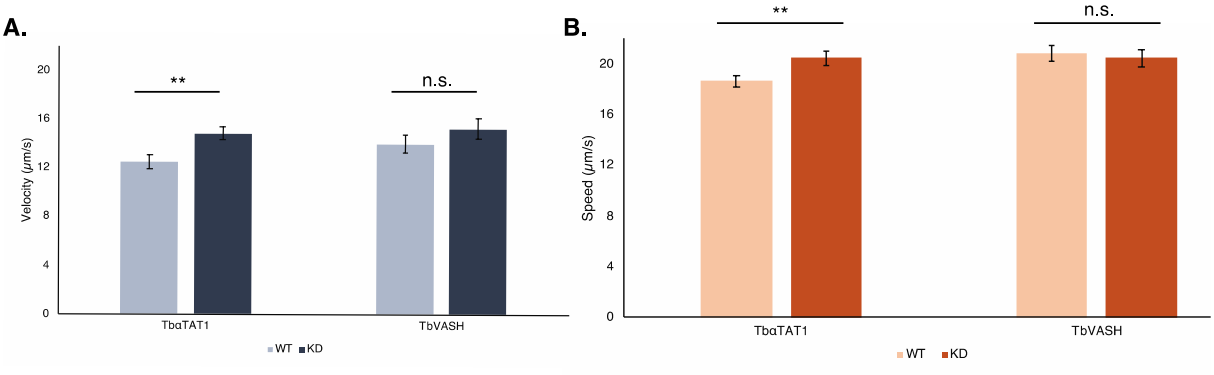

Figure 3.3: *TbαTAT1* and *TbVASH* knockdowns experience a similar increase in velocity but not speed. Average velocity (A.) and average speed (B.) of both uninduced and induced *TbαTAT1* (N = 183, 227) and *TbVASH* (N = 136, 126) cell lines. Error bars are SEM; statistical significance determined with unpaired t-test (** = $p \leq 0.01$, n.s. = $p \geq 0.1$)

Relative quantification of *T. brucei* motility defects are frequently observed through absorbance-based sedimentation assays.[26] The difference in absorbance at $\lambda = 600$ nm between a stirred and unstirred culture is calculated over several hrs to determine the rate of sedimentation while accounting for cell division.[26] We compared the sedimentation of uninduced/induced cultures of both *TbαTAT1* and *TbVASH* cell lines to wild type. Unexpectedly, the uninduced *TbαTAT1* and *TbVASH* cell lines had different sedimentation rates with *TbαTAT1* culture having the lowest (Figure 3.4). The average speed increase in induced *TbαTAT1* culture correlated with the sedimentation resistance observed over 6 hrs. Comparatively, *TbαTAT1* knock outs followed a similar resistance to sedimentation seen in the knockdowns. Additionally, the subtle increase in sedimentation observed in induced *TbVASH* culture correlates with the increase observed in *TbVASH* knock outs. Taken together, the significant increase in speed and velocity of *TbαTAT1* mutants correlates with resistance to sedimentation. However, changes observed in the motility of *TbVASH*

mutants were largely insignificant, indicating tubulin tyrosination has a minimal effect on motility compared to tubulin deacetylation.

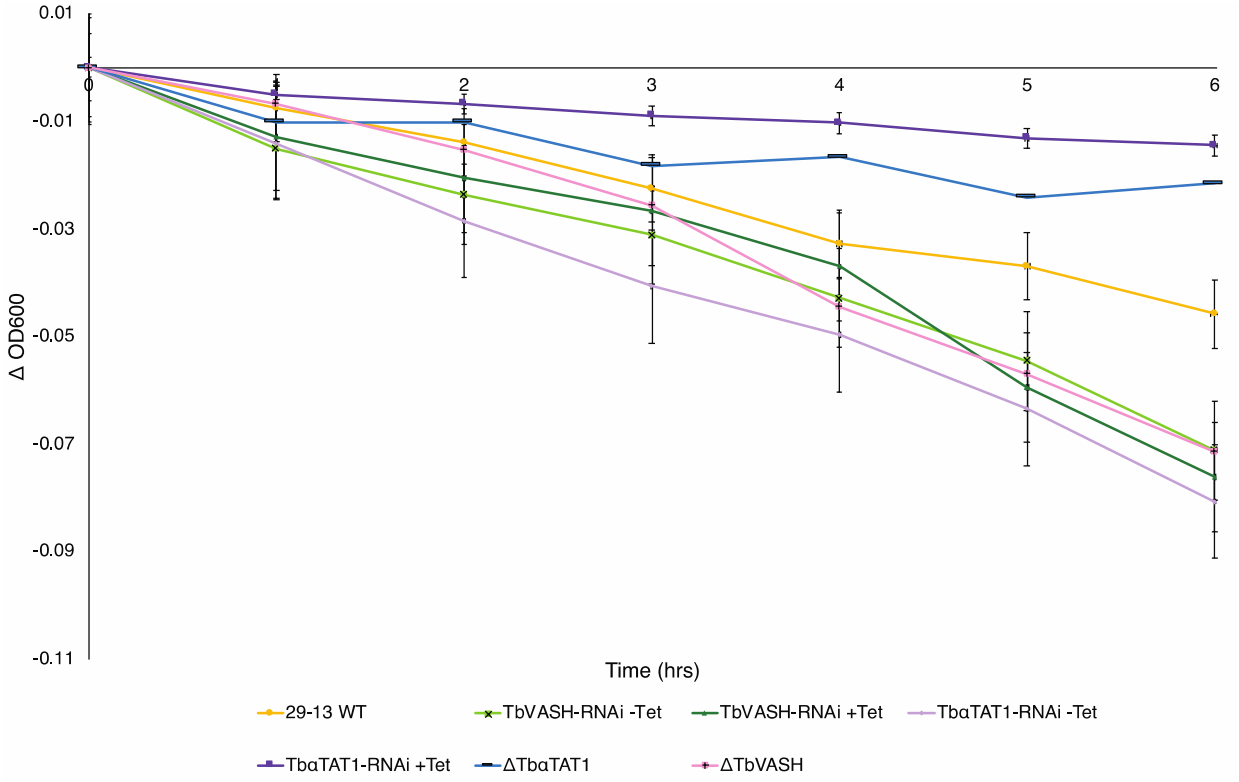

Figure 3.4: Cells deficient of *TbαTAT1*, but not *TbVASH*, are resistant to sedimentation. Change in absorbance at 600 nm of $1.0x10^6$ total cells over a 6 hour period. Error bars are SEM ($n = 3$)

CHAPTER FOUR

DISCUSSION

The goal of this study was to compare the effects of two different tubulin PTMs, acetylation and detyrosination, on the flagellar motility of *T. brucei*. We generated *TbαTAT1* and *TbVASH* knockdowns and knock outs, verified by the significant transcript and PTM reduction (>50%), and conducted *in vivo* whole cell motility phenotype characterization through single cell speed and velocity measurements and sedimentation assays.

TbαTAT1 knock downs had significantly increased average cell speed compared to wild type cells. The average speed, which considers the entire path length of the cell over a period of 10 seconds, was significantly increased when cells were grown in doxycycline (Figure 3.3B). Cellular motility direction is random, therefore, this ratio is dictated by intracellular chemotaxis responses from environmental cues, such as nutrient availability and pH changes.[27] A cell experiences higher run frequency when a positive chemotaxis signal is detected (i.e., high nutrient availability) and a higher tumble frequency when a negative chemotaxis signal is present (i.e., antibiotic).[27] With reduced tubulin acetylation, cells are primarily stuck in the "run" state, which contrasts with previously observed *in vitro* axonemal dynein exhibiting a reduction in velocity when exposed to deacetylated tubulin.[8] However, the activity of dynein is known to be primarily downregulated through tubulin PTMs, and our results support tubulin acetylation as a negative regulator of axonemal dynein motility.[8] This negative regulation is advantageous for the cell as it

minimizes unnecessary ATP consumption and mechanical stress on axonemal microtubules.[27]

Increased run frequency could potentially result in more effective pathogenesis.[27] PCF *T. brucei* cells can cause infection of a mammalian host by reproducing in the midgut of the fly vector and escaping to the ectoperitrophic space through the proventriculus.[22] With vigorous swimming and resistance to sedimentation, *TbαTAT1* induced cells would possibly struggle to colonize the gut epithelium and exit the digestive tract if the cells stay suspended in solution.[22] Additionally, increased swimming speeds could facilitate a faster escape to the proventriculus, but interfere with cell cycle timing.[48] *T. brucei* must change morphology during this escape, thus if the escape occurs too rapidly the transition from PCF to epimastigote might occur in the minority of the cell population, which could result in transmission to the mammalian host in a pre-BSF phenotype which would be lethal to the parasite.[48] Therefore, we conclude that *TbαTAT1* induced cells would be less effective at causing infection due to the inability to colonize the midgut of the fly vector.

TbVASH induced cells display a different and subtler phenotype: the average speed is decreased and the rate of sedimentation is slightly increased. As discussed previously, a decrease in average speed could indicate a higher rate of "tumbles," which given the life cycle of the PCF cells may be advantageous. Slightly higher tumbling rates and an increased likelihood of sedimentation would encourage gut epithelial colonization. However, to progress to the next life cycle stage, the parasite must travel to the salivary glands of the fly vector. This most likely requires the cell's motility to be intact, which

these results suggest may be decreased. We conclude that an increase in tyrosinated microtubules may not benefit PCF *T. brucei* culture, but may not inhibit midgut colonization as proposed with non-acetylated microtubules.

The results from this study support the evolutionary conservation and function tubulin acetylation and detyrosination in *T. brucei.* However, replicating these experiments in the bloodstream form would reveal pathogenic advantages or disadvantages unable to be discerned by these results. Additionally, confirmation of reduced fly vector colonization is only possible through experiments, such as those conducted by Van Den Abbeele *et al..*,[28] where the flies are infected with the modified parasite and cellular load and morphology are analyzed. Explicit characterization of flagellar waveforms has been conducted in few eukaryotic cell types and does not include many eukaryotic pathogens. Flagellar motility is one of the key virulence factors enabling *T. brucei*'s effectiveness as a pathogen. Therefore, quantifying the waveform of *T. brucei* and regulation of axonemal dynein will enable future studies on other motile pathogens. Additionally, mass spectrometry analysis of axonemal dynein in murine sperm cells indicated that the absence of glycylation (and subsequent increase in polyglutamylation) results in modified beta and gamma heavy chain domains in addition to uncoordinated dynein activity along the axoneme.[17] Glycylation has not been observed to directly impact the structure of dynein thus far; therefore, future studies of acetylation and detyrosination should include cryo-electron microscopy and mass spectrometry analysis.

CHAPTER FIVE

CONCLUSION

Here, we compared the effects of tubulin acetylation and detyrosination on the flagellar motility of *T. brucei* through *in vivo* experiments. We generated knockdowns and knock outs of the causative enzymes of acetylation and detyrosination, *TbαTAT1* and *TbVASH* respectively, and compared the motility of these cell lines to wild type *T. brucei* cells. Specifically, we recorded the average velocity and speed of >120 cells over 10 second intervals and found that both parameters are significantly increased in *TbαTAT1* knockdowns. Additionally, both *TbαTAT1* knockdowns and knockdowns are largely resistant to sedimentation over ~6 hrs, thus supporting the increased motility seen in individual cell tracks. This supports previous studies indicating tubulin acetylation negatively regulates the processivity of dynein, which leads to an unregulated, hyper flagellum.[8,10] However, removing the cell's ability to detyrosinate microtubules did not significantly impact speed or velocity, and the rate of sedimentation slightly increased, suggesting a minor motility defect. This suggests the importance of tubulin detyrosination is not directly related to motility, but rather cellular division or intracellular trafficking.

Our observations *in vivo* support the current understanding that dynein is negatively regulated by tubulin PTMs, especially acetylation. However, *in vitro* experiments with purified axonemal dynein from *T. brucei* on tubulin with varying ratios of acetylation and tyrosination could better support a dynein regulation mechanism. Additionally, conducting our *in vivo* study in bloodstream form parasites could translate the pathogenic impact of

our findings in procyclic from cells (specifically the ability of BSF parasites to navigate the bloodstream of the mammalian host). Overall, the results of this study have contributed to our understanding of the biological importance of tubulin PTM conservation in flagellated eukaryotes, such as *T. brucei*, and will support further investigation into the role of dynein regulation in cellular pathogenesis.

APPENDICES

Appendix A

RNAi plasmid construction and primers

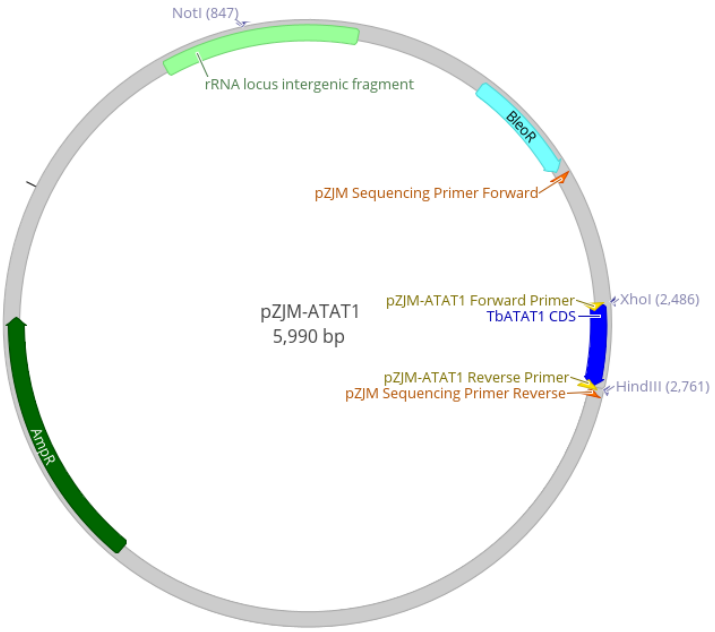

Figure A.1 pZJM-αTAT1 Plasmid Map

pZJM-αTAT1 features the phleomycin resistance cassette (light blue), ampicillin resistance cassette (dark green), rRNA spacer locus (light green), and *TbαTAT1* coding sequence PCR amplicon (dark blue). Amplicon primers for ligation into pZJM via XhoI/HindIII restriction sites (yellow) precede vector sequencing primers (orange). Annotation arrows are in the 5’ to 3’ direction.

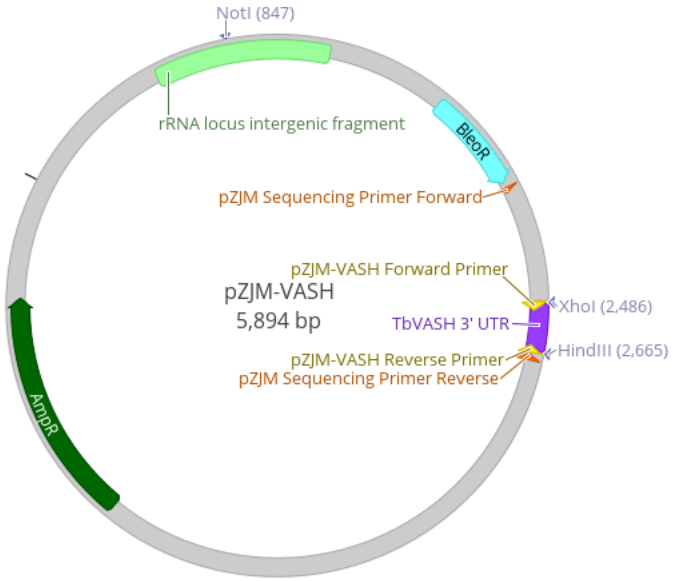

Figure A.2 pZJM-VASH Plasmid Map pZJM-VASH includes identical features from pZJM-αTAT1 with a substitution for the TbVASH 3' UTR PCR amplicon (purple). Annotation arrows are in the 5' to 3' direction.

Table A.1: BLAST ID of genes

Enzyme	Gene	Species	Putative *T. brucei* Homolog	% ID
αTAT1	C4B63_12g3321[1]	*Trypanosoma cruzi* Dm28c 2018	Tb927.3.1400	53
TTL	C3747_385g17	*T. cruzi* Dm28c 2018	Tb927.2.5250	66
VASH	C3747_9g248	*T. cruzi* TCC	Tb927.11.1060	49
SIR2	*sirt2*	*Homo sapiens*	Tb927.7.1690 (SIR2RP1)	36

Appendix B

CRISPR/Cas9 plasmid construction and primers

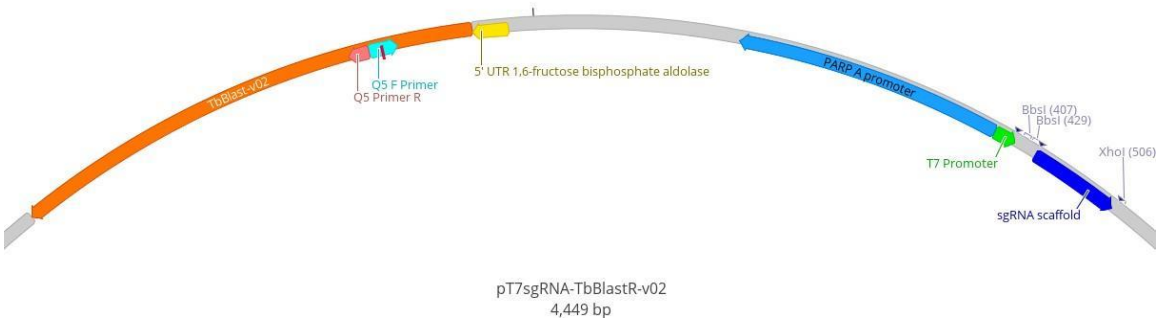

Figure B.1: pT7sgRNA-TbBlast Plasmid Map

pT7sgRNA-TbBlast features two resistance genes: the custom blasticidin resistance cassette for expression in *T. brucei* (orange) and the ampicillin resistance cassette for plasmid amplification (not shown). TbBlast-v02 is the second version of the gene after Q5 mutagenesis (primers denoted by red and light blue annotations with a red line denoting the nucleotide change.) The PARP A promoter sequence (blue) and 5'UTR for 1,6-fructose bisphosphate aldolase (yellow) are positioned upstream of the TbBlast cassette to ensure sufficient expression. *TbαTAT1* and *TbVASH* vectors were generated through target sequence ligation in between the T7 promoter (green) and sgRNA scaffold (dark blue) at the inverted repeat BbsI cut sites. Annotation arrows are in the 5' to 3' direction.

REFERENCES

1. Alonso, V. L., Carloni, M. E., Silva Goncalves, C., Martinez Peralta, G., Chesta, M. E., Pezza, A., Tavernelli, L. E., Machado Motta, M. C., & Serra, E. C. 2020. Alpha-tubulin acetylation in *Trypanosoma cruzi*: A dynamic instability of microtubules is required for replication and cell cycle progression [Preprint]. Cell Biology. https://doi.org/10.1101/2020.12.15.422917
2. Alsford, S., Kawahara, T., Isamah, C., Horn, D., 2007. A sirtuin in the African trypanosome is involved in both DNA repair and telomeric gene silencing but is not required for antigenic variation. Molecular Microbiology 63.. doi:10.1111/j.1365-2958.2006.05553.x
3. Garcia-Salcedo, J.A., 2003. A chromosomal SIR2 homologue with both histone NAD-dependent ADP-ribosyltransferase and deacetylase activities is involved in DNA repair in *Trypanosoma brucei*. The EMBO Journal 22, 5851–5862.. doi:10.1093/emboj/cdg553
4. Janke, C., Magiera, M.M., 2020. The tubulin code and its role in controlling microtubule properties and functions. Nature Reviews Molecular Cell Biology. doi:10.1038/s41580-020-0214-3
5. Center for Disease Control. Fact Sheet - African trypanosomiasis. Last reviewed: 9 March 2020. https://www.cdc.gov/parasites/sleepingsickness/index.html
6. Pollastri MP. Fexinidazole: A New Drug for African Sleeping Sickness on the Horizon. Trends Parasitol. 2018 Mar;34(3):178-179. doi:

10.1016/j.pt.2017.12.002. Epub 2017 Dec 20. PMID: 29275007; PMCID: PMC5828866.

7. Nicastro, Daniela & Schwartz, Cindi & Pierson, Jason & Gaudette, Richard & Porter, Mary & McIntosh, Richard. (2006). The Molecular Architecture of Axonemes Revealed by Cryoelectron Tomography. Science (New York, N.Y.). 313. 944-8. 10.1126/science.1128618.

8. Alper, Joshua D., Franziska Decker, Bernice Agana, and Jonathon Howard. The Motility of Axonemal Dynein Is Regulated by the Tubulin Code. Biophysical Journal 107, no. 12 (December 2014): 2872–80. https://doi.org/10.1016/j.bpj.2014.10.061.

9. Sasse, R., and Keith G., Tubulin Post-Translational Modifications and the Construction of Microtubular Organelles in *Trypanosoma Brucei*, J. Cell Sci. 1988. Aug;90 (Pt 4):577-89. doi:10.1242/jcs.90.4.577.

10. Portran, D., Schaedel, L., Xu, Z., Théry, M., Maxence, 2017. Tubulin acetylation protects long-lived microtubules against mechanical ageing. Nature Cell Biology.. doi:10.1038/ncb3481

11. McKenney, R. J., Huynh, W., Vale, R. D., & Sirajuddin, M. (2016). Tyrosination of α-tubulin controls the initiation of processive dynein–dynactin motility. The EMBO Journal, 35(11), 1175–1185. doi.org/10.15252/embj.201593071

12. Yao, D., Li, C., Jiang, J., Huang, J., Wang, J., He, Z., Zhang, J., 2020. Design, synthesis and biological evaluation of novel HDAC inhibitors with

improved pharmacokinetic profile in breast cancer. European Journal of Medicinal Chemistry 205, 112648.. doi:10.1016/j.ejmech.2020.112648

13. Sferra, A., Nicita, F., Bertini, E., 2020. Microtubule Dysfunction: A Common Feature of Neurodegenerative Diseases. International Journal of Molecular Sciences 21, 7354.. doi:10.3390/ijms21197354

14. Rico, E., Jeacock, L., Kovářová, J., & Horn, D. (2018). Inducible high-efficiency CRISPR-Cas9-targeted gene editing and precision base editing in African trypanosomes. Scientific Reports, 8(1), 7960. https://doi.org/10.1038/s41598-018-26303-w

15. Hirumi, H., & Hirumi, K. (1989). Continuous Cultivation of Trypanosoma brucei Blood Stream Forms in a Medium Containing a Low Concentration of Serum Protein without Feeder Cell Layers. The Journal of Parasitology, 75(6), 985-989. doi:10.2307/3282883

16. Geyer, V.F., Julicher, F., Howard, J., Friedrich, B.M., 2013. Cell-body rocking is a dominant mechanism for flagellar synchronization in a swimming alga. Proceedings of the National Academy of Sciences 110, 18058–18063.. doi:10.1073/pnas.1300895110

17. Gadadhar, S., Bodakuntla, S., Natarajan, K., & Janke, C. (2017). The tubulin code at a glance. Journal of Cell Science, 130(8), 1347–1353. https://doi.org/10.1242/jcs.199471

18. Godar, S., Oristian, J., Hinsch, V., Wentworth, K., Lopez, E., Amlashi, P., Enverso, G., Markley, S., Alper, J.D., 2022. Light chain 2 is a Tctex-type related

axonemal dynein light chain that regulates directional ciliary motility in Trypanosoma brucei. PLOS Pathogens 18, e1009984. doi:10.1371/journal.ppat.1009984

19. Aslett M, Aurrecoechea C, Berriman M, Brestelli J, Brunk BP, Carrington M, et al. TriTrypDB: a functional genomic resource for the Trypanosomatidae. Nucleic Acids Research. 2010;38: D457–1326D462. doi:10.1093/nar/gkp85

20. Schneider CA, Rasband WS, Eliceiri KW. NIH Image to ImageJ: 25 years of image analysis. Nat Methods. 2012;9: 671–675. doi:10.1038/nmeth.2089

21. Schindelin J, Arganda-Carreras I, Frise E, Kaynig V, Longair M, Pietzsch T, *et al.*. Fiji: an open-source platform for biological-image analysis. Nat Methods. 2012;9: 676–682. doi:10.1038/nmeth.201

22. Silvester, E., Mcwilliam, K., Matthews, K., The Cytological Events and Molecular Control of Life Cycle Development of *Trypanosoma brucei* in the Mammalian Bloodstream. Pathogens 2017. 6, 29.. doi:10.3390/pathogens6030029

23. Sement FM, Suematsu T, Zhang L, Yu T, Huang L, Aphasizheva I, *et al.*. Transcription initiation defines kinetoplast RNA boundaries. PNAS. 2018;115: E10323–E10332. doi:10.1073/pnas.1808981115

24. Brun R, Schönenberger M. Cultivation and in vitro cloning or procyclic culture forms of *Trypanosoma brucei* in a semi-defined

medium. Short communication. Acta Trop. 1979;36: 289–1499292. 150093.

25. Oberholzer M, Lopez MA, Ralston KS, Hill KL. Approaches for functional analysis of flagellar proteins in African trypanosomes. Methods Cell Biol. 2009;93. doi:10.1016/S0091-679X(08)93002-8

26. Bastin P, Pullen TJ, Sherwin T, Gull K. Protein transport and flagellum assembly dynamics revealed by analysis of the paralysed trypanosome mutant snl-1. J Cell Sci. 1999;112 (Pt 21): 3769–3777.

27. DeMarco, S. F., Saada, E. A., Lopez, M. A., & Hill, K. L. Identification of Positive Chemotaxis in the Protozoan Pathogen *Trypanosoma brucei*. MSphere. 2020. *5*(4), e00685-20. https://doi.org/10.1128/mSphere.00685-20

28. Van Den Abbeele, J., Caljon, G., De Ridder, K., De Baetselier, P., Coosemans, M., 2010. *Trypanosoma brucei* Modifies the Tsetse Salivary Composition, Altering the Fly Feeding Behavior That Favors Parasite Transmission. PLOS Pathogens 6, e1000926.. doi:10.1371/journal.ppat.1000926

29. Wang Z, Morris JC, Drew ME, Englund PT. Inhibition of *Trypanosoma brucei* Gene Expression by RNA Interference Using an Integratable Vector with Opposing T7 Promoters. J Biol Chem. 2000;275: 149240174–40179. doi:10.1074/jbc.M008405200

30. Lander, Ulrich, and Docampo, “Trypanosoma Brucei Vacuolar Transporter Chaperone 4 (TbVtc4) Is an Acidocalcisome Polyphosphate Kinase Required for in Vivo Infection.”

31. Livak KJ, Schmittgen TD. Analysis of Relative Gene Expression Data Using Real-Time Quantitative PCR and the 2−ΔΔCT Method. Methods. 2001;25: 402–408. doi:10.1006/meth.2001.126

32. Dean S, Sunter J. Light Microscopy in Trypanosomes: Use of Fluorescent Proteins and Tags. In: Michels PAM, Ginger ML, Zilberstein D, editors. Trypanosomatids: Methods and Protocols. New York, NY: Springer US; 2020. pp. 367–383. doi:10.1007/978-1-0716-0294-2_23

33. Alper J, Geyer V, Mukundan V, Howard J. Chapter Nineteen - Reconstitution of Flagellar Sliding. In: Marshall WF, editor. Methods in Enzymology. Academic Press; 2013. pp. 343–369. http://www.sciencedirect.com/science/article/pii/B9780123979452000196

34. Gorelik R, Gautreau A. Quantitative and unbiased analysis of directional persistence in cell migration. Nat Protoc. 2014;9: 1931–1943. doi:10.1038/nprot.2014.131

35. Yunger S, Rosenfeld L, Garini Y, Shav-Tal Y. Quantifying the transcriptional output of single alleles in single living mammalian cells. Nat Protoc. 2013;8: 393–408. doi:10.1038/nprot.2013.0081534107.

36. Sage D, Neumann FR, Hediger F, Gasser SM, Unser M. Automatic tracking of individual fluorescence particles: application to the study of

chromosome dynamics. IEEE Transactions on Image
1536 Processing. 2005;14: 1372–1383. doi:10.1109/TIP.2005.852787

37. Nussbaum-Krammer CI, Neto MF, Brielmann RM, Pedersen JS, Morimoto RI. Investigating the Spreading and Toxicity of Prion-like Proteins Using the Metazoan Model Organism C. elegans. JoVE (Journal of Visualized Experiments). 2015; e52321. doi:10.3791/52321

38. Sbalzarini IF, Koumoutsakos P. Feature point tracking and trajectory analysis for video imaging in cell biology. J Struct Biol. 2005;151: 182–195. doi:10.1016/j.jsb.2005.06.002

39. Sun, S.Y., Kaelber, J.T., Chen, M., Dong, X., Nematbakhsh, Y., Shi, J., Dougherty, M., Lim, C.T., Schmid, M.F., Chiu, W., He, C.Y., 2018. Flagellum couples cell shape to motility in *Trypanosoma brucei*. Proceedings of the National Academy of Sciences 115, E5916–E5925.. doi:10.1073/pnas.1722618115

40. Sinclair, A.N., Huynh, C.T., Sladewski, T.E., Zuromski, J.L., Ruiz, A.E., De Graffenried, C.L., 2021. The *Trypanosoma brucei* subpellicular microtubule array is organized into functionally discrete subdomains defined by microtubule associated proteins. PLOS Pathogens 17, e1009588.. doi:10.1371/journal.ppat.1009588

41. Mugnier, M.R., Stebbins, C.E., Papavasiliou, F.N., 2016. Masters of Disguise: Antigenic Variation and the VSG Coat in *Trypanosoma brucei*. PLOS Pathogens 12, e1005784.. doi:10.1371/journal.ppat.1005784

42. Jean Rodgers, Barbara Bradley, Peter G.E. Kennedy, Delineating neuroinflammation, parasite CNS invasion, and blood-brain barrier dysfunction in an experimental murine model of human African trypanosomiasis, Methods, (2017) 127: 79-87 https://doi.org/10.1016/j.ymeth.2017.06.015.

43. Walton, T., Wu, H., Brown, A., 2021. Structure of a microtubule-bound axonemal dynein. Nature Communications 12.. doi:10.1038/s41467-020-20735-7

44. Eshun-Wilson, L., Zhang, R., Portran, D., Nachury, M.V., Toso, D.B., Löhr, T., Vendruscolo, M., Bonomi, M., Fraser, J.S., Nogales, E., 2019. Effects of α-tubulin acetylation on microtubule structure and stability. Proceeding of the National Academy of Sciences.. doi:10.1073/pnas.1900441116

45. Bellofatto V, Palenchar JB. RNA interference as a genetic tool in trypanosomes. Methods Mol Biol. 2008;442:83-94. doi: 10.1007/978-1-59745-191-8_7. 9PMID: 18369780.

46. Beneke, T., Madden, R., Makin, L., Valli, J., Sunter, J., & Gluenz, E. (2017). A CRISPR Cas9 high-throughput genome editing toolkit for kinetoplastids. Royal Society Open Science, 4(5), 170095. https://doi.org/10.1098/rsos.170095

47. Peacock L, Cook S, Ferris V, Bailey M, Gibson W. The life cycle of *Trypanosoma* (Nannomonas*) congolense* in the tsetse fly. Parasit Vectors. 2012 Jun 27;5:109. doi: 10.1186/1756-3305-5-109. PMID: 22676292; PMCID: PMC3384477.

48. Rose C, Casas-Sánchez A, Dyer NA, Solórzano C, Beckett AJ, Middlehurst B, Marcello M, Haines LR, Lisack J, Engstler M, Lehane MJ, Prior IA, Acosta-Serrano Á. Trypanosoma brucei colonizes the tsetse gut via an immature peritrophic matrix in the proventriculus. Nat Microbiol. 2020 Jul;5(7):909-916. doi: 10.1038/s41564-020-0707-z. Epub 2020 Apr 20. PMID: 32313202.

49. van der Laan S, Lévêque MF, Marcellin G, Vezenkov L, Lannay Y, Dubra G, Bompard G, Ovejero S, Urbach S, Burgess A, Amblard M, Sterkers Y, Bastien P, Rogowski K. Evolutionary Divergence of Enzymatic Mechanisms for Tubulin Detyrosination. Cell Rep. 2019 Dec 17;29(12):4159-4171.e6. doi: 10.1016/j.celrep.2019.11.074. PMID: 31851940.